

DESIGN OF A FIGURE-8 UNDULATOR FOR ELETTRA

B. Diviacco, R. Bracco, D. Millo, D. Zangrando, SINCROTRONE TRIESTE, Italy

1 INTRODUCTION

The requirements of a low photon energy undulator source operating on a relatively large energy storage ring like ELETTRA are inevitably associated with high emitted power and therefore significant heat load on the beamline optical components. In order to overcome this problem, a figure-8 undulator [1, 2] has been designed and is being constructed for the new Inelastic Ultra-Violet Scattering Beamline. The magnetic structure (see figure 1) consists of six permanent magnet arrays producing a vertical field component of period λ_0 and a horizontal field component of period $2\lambda_0$.

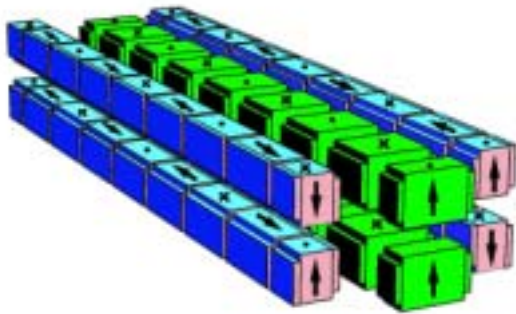


Figure 1: Structure of the Figure-8 undulator

Optimised for photon energies between 5 and 10 eV, it will generate linearly polarised radiation with low on-axis power density, thus enabling efficient power filtering by means of a suitably sized pinhole. The general radiation power and spectral properties of this device have already been reported in a previous paper [3]. In this article the undulator structure is described in more detail, together with measurement results on a short prototype. Finally the methods that will be used for field error correction on the final device are briefly discussed.

2 THE MAGNETIC STRUCTURE

Due to the unconventional geometry, a detailed study of the magnetic structure was performed in order to optimise the important parameters. The permanent magnet material used is NdFeB with a remanent field of 1.3 T. The period length and vertical field amplitude were determined based on the required minimum photon energy (5 eV at 2 GeV) and the maximum allowed total emitted power. The horizontal field strength was optimised to have a sufficient suppression of the central power density without excessive growth of the first half-integer spectral harmonic, that would be difficult to filter-off and harmful to the

experiments. This resulted in the following set of parameters:

Table 1: Main undulator parameters

period length	140 mm
total number of periods	32
minimum gap	19 mm
B _{x0} , B _{y0} (T) at minimum gap	0.13, 0.72
Deflection parameters K _x , K _y	3.6, 9.7
Central power density*	40 W/mrad ²
Total power*	2700 W

* for a beam energy of 2 GeV and nominal current of 400 mA

Effects arising from the non-unit permeability of the magnetic material were also studied by means of a RADIA [4] model, in which typical values for NdFeB ($\mu_{||}=1.05$, $\mu_{\perp}=1.2$) were used. The results showed a significant effect in terms of field integrals (see figure 2), much larger than for a conventional undulator, and localised at the terminations where the symmetry of the periodic structure is broken. This 'intrinsic' multipole will likely not be distinguishable from other random errors inevitably introduced by magnetisation strength, direction and inhomogeneity variations in a real device, and will be compensated with the techniques described in section 4. However, understanding its origin and localisation is useful in order to apply the most appropriate correction.

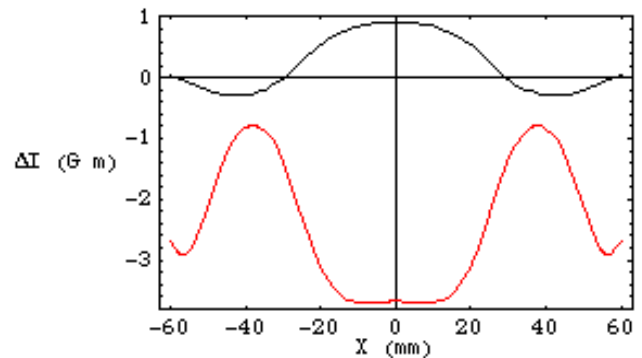


Figure 2: Computed horizontal (red) and vertical (black) field integral distribution due to non-unit permeability.

It is well known that more sophisticated termination schemes than the simple half-block used in our case could significantly mitigate this effect. However, the latter presents a number of advantages. First, it minimises the amount of unwanted fringe-field radiation that would spoil the intrinsic low on-axis power density. Second, it provides a simple and effective way of phasing multi-segment devices.

3 SEGMENTATION

For practical reasons, the undulator will be segmented in two independent units, each approximately 2.3 m in length (16 periods). In order not to compromise the spectral output, a solution was devised that consists in allowing a small separation (~ 1 mm) between the centre arrays of the two modules, while the side arrays are displaced in opposite directions in the upstream and downstream undulator, as illustrated in figure 3.

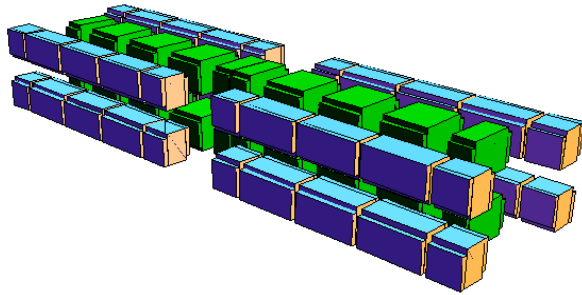


Figure 3: Schematic of a two-segment undulator.

In this way, almost perfect periodicity is maintained for the (stronger) vertical field component, while the discontinuity in the (weaker) horizontal field only causes a marginal effect on the radiation spectrum (see figures 4 and 5).

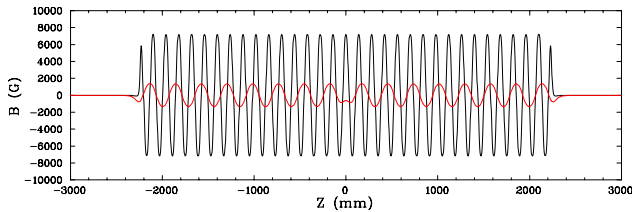


Figure 4: Computed Horizontal (red) and vertical (black) magnetic field in the two-segment device.

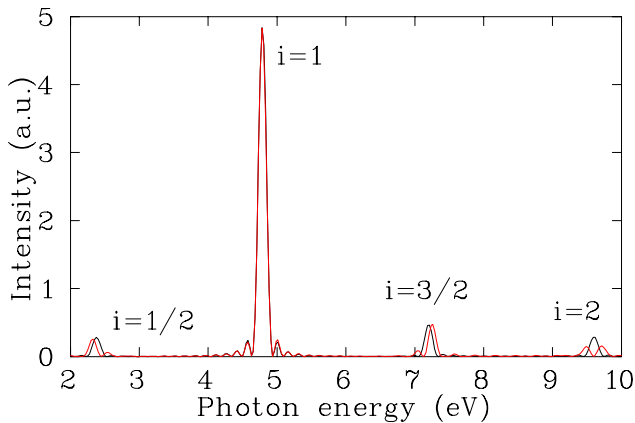


Figure 5: Computed spectrum for the two-segment undulator (red) and an equivalent single device (black).

As a consequence of the opposite phasing of the field components in the two segments, the asymmetric angular radiation pattern characteristic of the figure-8 undulator [1, 2, 3] is changed to a symmetric distribution (see figure 6), which is beneficial for photon beam alignment purposes. Calculation of the polarisation properties of the emitted radiation showed that the linear degree of polarisation is preserved in the compound undulator, with negligible loss of performance compared to a single segment device.

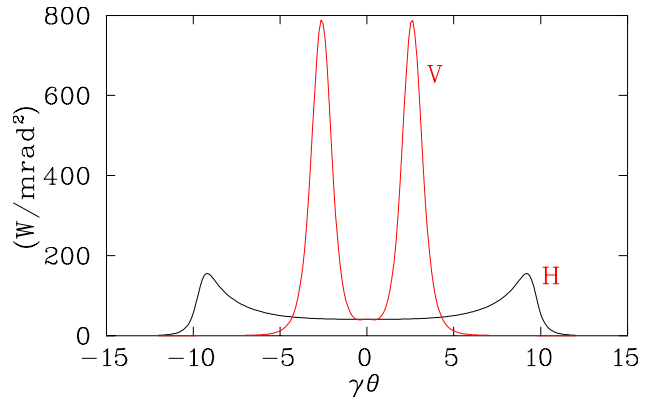


Figure 6: Angular distribution of the power density in the horizontal (black) and the vertical plane (red).

4 PROTOTYPE

Following delivery of the permanent magnet blocks (Vacodym 521 TP, Vacuumschmelze), a short two-period prototype was built in order to check the properties of the magnetic field. Since the variable gap support structures are presently under construction, only the lower half of the structure could be measured (see figure 7). However, this was sufficient to verify that the field distribution and the related trajectory agree well with model calculations (see figure 8).



Figure 7: Two-period prototype undergoing magnetic measurements

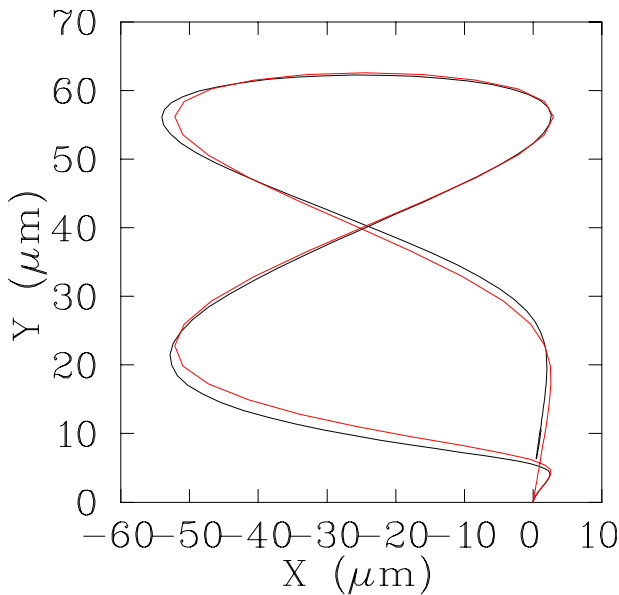


Figure 8 Transverse trajectory computed from the measured (black) and ideal (red) magnetic field of the short prototype.

5 FIELD ERROR CORRECTION

Similar to what was done with previous undulators built at ELETTRA, all the permanent magnet blocks were characterised by means of a Helmholtz-coil system, and found to be within the specified maximum block to block dipole moment variation of $\pm 1\%$ and maximum deviation from the nominal magnetisation direction of 1° . Based on the measurement data, an appropriate sorting algorithm has been developed in order to limit the amount of random field and trajectory errors in the assembled device. However, measurement errors and volume inhomogeneity in the magnetic material will ultimately limit the obtainable field quality. During the past years, a number of methods have been developed for post-assembly correction of insertion devices, including the use of ferromagnetic shims, or the application of small extra permanent magnets at suitable locations. In our case, the most promising approach consists in displacing a few selected blocks from their nominal position. This technique (also known as 'virtual shimming') is based on the computed effect of the horizontal or vertical shifting of a magnet in each array. By linear superposition of the individual 'signatures' (in terms of longitudinal on-axis field and transverse field integral distributions) the field perturbation can be computed for any arbitrary combination of displacements. An example is shown in figure 9, showing the effect on the field integrals when displacing various combinations of vertically magnetised blocks in the different arrays. Great flexibility is achieved in obtaining different distributions and therefore in correcting a large class of possible residual field errors. This same method has already been successfully applied to

the elliptical undulators based on the APPLE-II design [5, 6] and its application to the figure-8 structure should be straightforward.

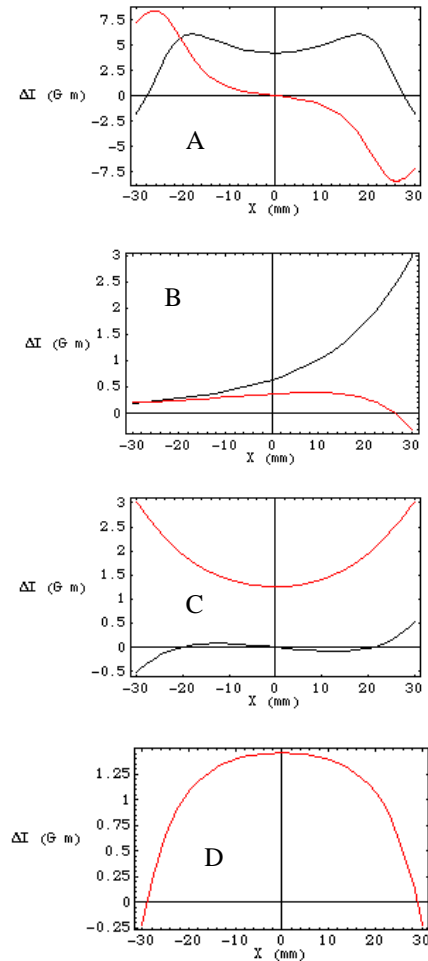


Figure 9: Horizontal (red) and vertical (black) field integrals arising from a 1 mm displacement of:

- A: one block in the central array ($\Delta y=1$ mm)
- B: one block in the side array ($\Delta y=1$ mm)
- C: two blocks in the side arrays ($\Delta x=1$ mm)
- D: four blocks in the side arrays ($\Delta y=1$ mm)

6 REFERENCES

- [1] T. Tanaka, H. Kitamura, Nucl. Instr. and Meth. in Phys. Res. A 364 (1995) pag. 368.
- [2] T. Tanaka, H. Kitamura, J. Synchrotron Rad. (1996) 3, pag. 47.
- [3] B. Diviacco et al., Proc. 2001 PAC Conference, pag. 2468.
- [4] RADIA is a public domain software developed by the ESRF Insertion Devices Group.
- [5] S. Marks et. al., Proc. 1999 PAC Conference, pag. 162.
- [6] B. Diviacco et al., proc. 2000 EPAC Conference, pag 2322.